Dynamic Soaring in Shear Wind Regions Associated with Jet Streams

Gotfried Sachs and Orlando da Costa[1]
Technische Universität München
Boltzmannstr. 15, 85747 Garching, Germany
sachs@lfm.mw.tum.de

Presented at the XXVIII OSTIV Congress, Eskilstuna, Sweden, 8-15 June 2006

Abstract

Dynamic soaring enables an energy gain by transferring energy from the moving air in a horizontal shear wind region to the saiplane. There are shear wind regions associated with jet streams, extending from the jet stream core with its high wind speed to the altitude where the air is at rest. The possibility of utilizing this energy gain is considered for the dynamic soaring of sailplanes. An efficient optimization procedure is used to determine the minimum shear wind strength which is required for the dynamic soaring flight manoeuvre, applying a realistic mathematical model for describing the dynamics of a sailplane. It turns out that the minimum shear wind strength is smaller than the values which can be encountered in existing shear wind regions associated with jet streams. As a result, the performance capability of modern sailplanes offers the possibility for dynamic soaring in these jet stream regions.

[1] Now with IABG mbH, Einsteinstraße 20, D-85521 Ottobrunn, Germany.

Nomenclature

a_{ki}	coefficient
C_D	drag coefficient
C_L	lift coefficient
D	drag
g	acceleration due to gravity
h	altitude
L	lift
m	mass
n	load factor
$\bar{q}$	dynamic pressure, $\bar{q} = (\rho/2)V^2$
S	reference area
t	time
u_{Kg}, v_{Kg}, w_{Kg}	speed components
V	airspeed
V_K	inertial speed
V_W	wind speed
x_g, y_g, z_g	geodetic coordinate system
χ_a	flight azimuth angle
γ_a	flight path wind angle
μ_a	flight bank wind angle
ρ	density

Introduction

Dynamic soaring is a flight technique by which a flying object (bird, sailplane) can extract energy from the moving air in a horizontal wind field which changes its strength with altitude. This type of air flow is called shear wind. Dynamic soaring consists of a series of cycles which are continually repeated, as shown in Fig. 1 for a seabird. A cycle which forms the basic constituent of dynamic soaring comprises a complex sequence of climbing, turning and descending flight phases (denoted by Nos. 1 to 4 in Fig. 1). Dynamic soaring earlier has attracted attention as a flight technique for achieving an energy gain from shear wind[1-3]. Since then, it is a subject of continuous interest[4-21].

Dynamic soaring is practiced by seabirds, in particular by albatrosses, enabling them to stay aloft without flapping. With this flight technique, the birds can travel large distances. With respect to the possibility of an energy gain from the shear wind, dynamic soaring is also an issue for sailplanes[4-22]. Using energy estimations and numerical simulations, significant knowledge about the shear wind strength necessary for dynamic soaring has been gained. With the availability of modern optimization techniques, it was possible to achieve precise results on dynamic soaring trajectories and on the maximum energy gain which can be obtained from the shear wind[18-22]. The results show that the performance characteristics of modern sailplanes offer the possibility of dynamic soaring in shear wind fields.

Recent developments in the soaring techniques of model gliders are of interest for the problem under consideration[23-27]. This is because model glider pilots have practiced dynamic soaring for some time. They use wind conditions at ridges where significant shear flows can exist.

The purpose of this paper is concerned with the possibility of dynamic soaring in the shear wind regions of jet streams for high-performance sailplanes. Focus is on dynamic soaring trajectories requiring the minimum shear wind strength. Thus, it is possible to judge whether the performance capability of

modern sailplanes is sufficient for dynamic soaring in these shear wind conditions.

Shear wind regions associated with jet streams

There are various causes for the occurrence of horizontal shear winds[28]. One concerns the air flow over the surface of sea or land. This type of shear flow at sea holds for the dynamic soaring of seabirds. There is a shear wind due to boundary layer effects of the moving air close to the surface of the water. The wind speed rapidly increases from zero or very small values immediately above the sea surface until approaching the value of the free air flow. Another cause for a shear wind is due to ridges. A wind coming over the top of a ridge produces a shear wind condition behind the ridge where a separation boundary between the wind area and a zone of still air exists. Such shear winds are used by model gliders for dynamic soaring.

There is also a shear wind associated with jet streams. The shear wind extends in a range between the core of the jet stream with its extremely high wind speed and the altitude where the air is at rest or moving slowly. Results are presented in Fig. 2 which shows measured data of the shear wind region associated with a jet stream. The data presented in Fig. 2 suggest for a large part of the altitude range that a linear dependence of the wind speed with the altitude can be used as a realistic mathematical model for describing the shear wind characteristics. In this region, the shear wind gradient amounts to a value of about $\mathrm{d}V_W/\mathrm{d}h = 0.019\,\mathrm{s}^{-1}$.

The shear wind regions associated with jet streams cover wide areas and extend over huge distances. An example is presented in Fig. 3. Since the jet streams are continually monitored, it is well known where such shear wind regions occur.

The shear wind regions associated with jet streams are at higher altitudes (Fig. 2). For flying at high altitudes, it necessary to have an appropriate equipment for coping with the atmospheric conditions (oxygen, pressure, temperature)[31].

Mathematical model for sailplane dynamics in a shear wind

The mathematical model for describing the motion of the sailplane in the horizontally moving air of a shear wind field can be based on point mass dynamics. Reference is made to an earth-fixed coordinate system and an appropriate inclusion of the moving air (Fig. 4). With respect to this coordinate system, the equations of motion can be formulated as

$$\begin{aligned}
\mathrm{d}u_{Kg}/\mathrm{d}t &= -a_{u1}D/m - a_{u2}L/m \\
\mathrm{d}v_{Kg}/\mathrm{d}t &= -a_{v1}D/m - a_{v2}L/m \\
\mathrm{d}w_{Kg}/\mathrm{d}t &= -a_{w1}D/m - a_{w2}L/m + g \\
\mathrm{d}x_{Kg}/\mathrm{d}t &= u_{Kg} \\
\mathrm{d}y_{Kg}/\mathrm{d}t &= v_{Kg} \\
\mathrm{d}h/\mathrm{d}t &= -w_{Kg}
\end{aligned} \tag{1}$$

where the coefficients a_{ij} are given by

$$\begin{aligned}
a_{u1} &= \cos\gamma_a \cos\chi_a \\
a_{u2} &= \cos\mu_a \sin\gamma_a \cos\chi_a + \sin\mu_a \sin\chi_a \\
a_{v1} &= \cos\gamma_a \sin\chi_a \\
a_{v2} &= \cos\mu_a \sin\gamma_a \sin\chi_a - \sin\mu_a \cos\chi_a \\
a_{w1} &= -\sin\gamma_a \\
a_{w2} &= \cos\mu_a \cos\gamma_a
\end{aligned} \tag{2}$$

The lift and drag forces, L and D, are dependent on the airspeed vector $\vec{V}$, concerning their magnitude and direction of action, while the motion of the aircraft with respect to the earth is described by the inertial speed vector $\vec{V}_K$ (Fig. 4). Using the wind speed vector $\vec{V}_W$, the following relation holds

$$\vec{V} = \vec{V}_K - \vec{V}_W \tag{3}$$

Since the x_g axis is selected such that is parallel to the horizontal wind (Fig 4), the wind speed vector is given by

$$\vec{V}_W = (V_W, 0, 0)^{\mathrm{T}} \tag{4}$$

With the inertial speed vector

$$\vec{V}_K = (u_{Kg}, v_{Kg}, w_{Kg})^{\mathrm{T}} \tag{5}$$

the following expressions can be obtained

$$\begin{aligned}
\vec{V} &= (u_{Kg} + V_{W,} v_{Kg,} w_{Kg})^{\mathrm{T}} \\
V &= \sqrt{(u_{Kg} + V_W)^2 + v^2{}_{Kg} + u^2_{Kg}}
\end{aligned} \tag{6}$$

The angles χ_a, γ_a and μ_a describe the orientation of the aerodynamic forces with respect to the inertial reference system. The following relations hold for χ_a and γ_a:

$$\begin{aligned}
\sin\gamma_a &= -\frac{w_{Kg}}{V} \\
\tan\chi_a &= \frac{v_{Kg}}{u_{Kg} + V_W}
\end{aligned} \tag{7}$$

The angle μ_a which describes the banking of the lift vector is a control. Thus, it is determined by optimality conditions.

The mathematical model for describing the dynamics of the sailplane also concerns constraints which are given by

$$\begin{aligned}
n_{\min} \le n \le n_{\max} \\
\bar{q} \le \bar{q}_{\max}
\end{aligned} \tag{8}$$

The density properties of the atmosphere are described using a model based on data given in Ref. 32.

Using the above equations of motion, dynamic soaring trajectories in a shear wind region can be determined such that the energy state after completing a cycle as shown in Fig. 1 is the same as at the beginning. These trajectories can be designated as energy-neutral. This implies that the speed vectors (by amount and direction) at the beginning and end of a dynamic soaring cycle are equal as well as the corresponding altitudes. There is a great variety of energy-neutral trajectories, requiring different values of the wind gradient $\mathrm{d}V_W/\mathrm{d}h$. One is of concern for the issue in mind: It is the one which requires the minimum shear wind strength in terms of the min-

imum gradient $(\mathrm{d}V_W/\mathrm{d}h)_{\min}$. Knowing this energy-neutral trajectory, it is possible to judge whether or not the strength of the shear wind associated with a jet stream is sufficient for dynamic soaring.

The energy-neutral trajectory requiring the minimum shear wind gradient can be determined using techniques for flight path optimization. Flight path optimization is a systematic, purposeful search strategy such that the best dynamic soaring trajectory can be computed which yields the maximum energy gain from the shear wind. Thus, the dynamic soaring trajectory can be determined which requires the minimum shear wind strength. Efficient numerical optimization methods and computational techniques are necessary to solve the described trajectory optimization problem. The numerical investigation was performed using a parameterization optimization technique[33] with a graphical environment[34].

Mathematical model of sailplane

Data of a high-performance sailplane are used in the numerical investigation for determining the optimal dynamic soaring trajectory requiring the minimum shear wind gradient $(\mathrm{d}V_W/\mathrm{d}h)_{\min}$. It is similar to the Eta sailplane in its aerodynamics and size characteristics[35].

The following data are applied for the reference wing area and the mass:

$$S = 18.6 \text{ m}^2$$

$$m = 975 \text{ kg}$$

The aerodynamic model concerns the lift and drag characteristics of the sailplane. The lift and drag can be expressed as

$$L = C_L(\rho/2)V^2S$$
$$D = C_D(\rho/2)V^2S \qquad (9)$$

The lift-drag characteristics of the sailplane are presented in Fig. 5 which shows the C_L/C_D ratio with regard to the speed range. The depicted data also include the effect of camber flaps the control of which can be used to improve the performance. The utilization of the camber flaps was also included in the optimization of dynamic soaring such that the best setting of the camber flaps for each flight phase was selected by the computational procedure.

Further on the aerodynamics model, limits in the lift coefficient were accounted for. For this purpose, the following relationship was applied

$$C_{L\min} \le C_L \le C_{L\max} \qquad (10)$$

Results

For determining the energy-neutral dynamic soaring trajectory requiring the minimum shear wind strength in terms of the minimum wind gradient, a shear wind model with a linear dependence of the wind speed with the altitude was applied, as suggested by the data presented in Fig. 2. In the computational process, the gradient of the wind speed with respect to the altitude $(\mathrm{d}V_W/\mathrm{d}h)$ was not held fixed at a given value, but it was treated as adaptable such that the lowest possible value in terms of the minimum gradient $(\mathrm{d}V_W/\mathrm{d}h)_{\min}$ was determined using the optimization technique described in a previous section. Results on the related optimal energy-neutral dynamic soaring trajectory requiring the minimum shear wind gradient $(\mathrm{d}V_W/\mathrm{d}h)_{\min}$ are presented in the following.

As a main result, the minimum shear wind gradient required for dynamic soaring with the sailplane the mathematical model of which was presented in the previous section amounts to

$$(\mathrm{d}V_W/\mathrm{d}h)_{\min} = 0.012 \text{ s}^{-1}$$

Comparison to the measured shear wind data with $\mathrm{d}V_W/\mathrm{d}h = 0.019 \text{ s}^{-1}$ (Fig. 2) shows that required minimum shear wind gradient is significantly smaller.

Properties of the optimal dynamic soaring trajectory with which requires the minimum shear wind gradient $(\mathrm{d}V_W/\mathrm{d}h)_{\min} = 0.012 \text{ s}^{-1}$ are graphically illustrated in the following figures.

A cycle of the optimal energy-neutral dynamic soaring trajectory is shown in Fig. 6. This figure provides a perspective view of the dynamic soaring cycle and gives its extension in the longitudinal, lateral and vertical directions. The dotted arrows denote the beginning and ending of a cycle which is periodically repeated. The time required for the optimal energy-neutral dynamic soaring cycle amounts to $t_{cyc} = 37.1 \text{ s}$.

The time history of the altitude is presented in Fig. 7. The altitude covers a range of less than 700 m, in the upper part of the shear wind region. The climb is performed in a windward direction while the descent is a flight with the wind. The turns are conducted at the top and the bottom of the altitude range.

The fact that the altitude range is less than 700 m is important with regard to the possibility of utilizing the shear wind region associated with jet streams for dynamic soaring. This is because there may be only a small part needed out of the entire altitude region showing a shear wind gradient. For example, the shear wind altitude region of the jet stream case presented in Fig. 2 amounts to nearly 4 km.

The time histories of the speed with respect to the earth, V_K, and the airspeed, V, are presented in Fig. 8. During the climb, V is larger than V_K because of the windward flight direction. The opposite holds for the descent which shows a leeward flight direction. The change in the relation between V_K and V is an indication for the increase of V_K in the upper turn. The increase of V_K can be seen in Fig. 8 when comparing two V_K values at the same altitude, one before and the other after the maximum altitude (Fig. 7). The increase of V_K leads to an enlargement of the kinetic energy. The overall energy of the sailplane is accordingly increased because the

two altitude values correspond to the same potential energy. Since the increase of the energy state is due to the upper turn, this flight phase can be qualified as most important for the energy gain of dynamic soaring.

In Fig. 9, the time histories of the lift coefficient C_L and the bank angle μ_a which are the controls are presented. The lift coefficient C_L takes on large values in the upper turn. In the lower turn, C_L shows smaller values. The bank angle μ_a shows its largest values in the turns. Here, the values of μ_a are around ±50 deg, with some more banking in the upper turn.

The time history of the load factor n is depicted in Fig. 10. For a large part of the dynamic soaring cycle, the load factor is close to $n=1$. There is an increase in the lower turn where the sailplane changes its direction from lee- to windward and the inertial speed takes on its highest values. Here, the increase of n reaches the limit $n_{\max}=4.5$ so that the constraint given by Eq. (8) becomes active.

Conclusions

There are shear wind regions associated with jet streams, covering wide areas and extending over huge distances. The possibility of utilizing these regions for dynamic soaring is investigated. For this purpose, energy-neutral dynamic soaring trajectories are determined which require the smallest shear wind strength in terms of the minimum wind gradient with respect to the altitude. It turns out that modern sailplanes with a high aerodynamic efficiency need shear wind gradients which are smaller than those of existing shear winds. As a result, high-performance sailplanes offer the possibility to conduct dynamic soaring in shear wind regions associated with jet streams.

References

[1]Rayleigh, J.W.S., "The Soaring of Birds", *Nature* 27, pp. 534-535, 1883.

[2]Idrac, P., "Étude théorique des manœuvres des albatros par vent croissant avec l'altitude", *C.r. hebd. Séanc. Acad. Sci*., Paris 179: 1136-1139, 1924.

[3]Prandtl, L., „Beobachtungen über den dynamischen Segelflug", *Zeitschrift für Flugtechnik und Motorluftschifffahrt*, 21. Jahrg., p. 116, 1930.

[4]Klemperer, W., "A Review on the Theory of Dynamic Soaring", *OSTIV-Bericht*, pp. 498-501, 1958.

[5]Contensou, P., "Optimization du Vol Plane dans un Vent Horizontal Variable", *Congress of Appl. Mechanics*, Stanford University, 1968.

[6]Fritsch, E., „Zum dynamischen Segelflug", *Aero-Revue*, Heft 12, pp. 669-672, 1971, Heft 1, p. 40, 1972.

[7]Hendriks, F., "Dynamic Soaring", *Dissertation*, University of California, Los Angeles, 1972.

[8]Hendriks, F., "Dynamic Soaring in Shear Flow", *AIAA Paper 74-1003*, 1974.

[9]Trommsdorff, W., „Flugmechanische und technische Voraussetzungen für den Dynamischen Segelflug mit bemanntem Fluggerät", *OSTIV-Bericht*, 1974.

[10]Trommsdorff, W., „Voraussetzungen für die Durchführung des dynamischen Segelflugs", *Aerokurier*, Heft 12, pp. 1106-1107, 1976.

[11]Renner, I., „Dynamischer Segelflug", *Aerokurier*, Heft 12, pp. 1104-1105, 1976.

[12]Gorisch, W., "Energy Exchange between a Sailplane and Moving Air Masses under Instationary Flight Conditions with Respect to Dolphin Flight and Dynamic Soaring", *Aero-Revue*, Heft 11, pp. 691-692 (Teil 1), Heft 12, pp. 751-752 (Teil 2), 1976, Erratum, Heft 3, p. 182, 1977.

[13]Gorisch, W., „Zum Problem des dynamischen Segelflugs in der horizontalen Grenzschicht zwischen ruhender und bewegter Luftmasse", *Aerokurier*, Heft 9, pp. 855-858, 1977.

[14]Nottebaum, T., „Ein Rechenprogramm zur Simulation des Dynamischen Segelflug", *DGLR-Jahrbuch*, pp. 329-338, 1987.

[15]Goebel, O., „Scherwindmessungen an Bord einer Piper PA 18 und Auslegung eines Modellsegelflugzeugs für den Dynamischen Segelflug", *DGLR-Jahrbuch*, pp. 322-328, 1987.

[16]Nottebaum, T., „Goebel, O., Simulation optimaler Flugbahnen des dynamischen Segelflugs und Auslegung eines Modellflugzeugs", *Zeitschrift für Flugwissenschaften und Weltraumforschung*, Vol. 13, pp. 48-56, 1989.

[17]Lissaman P, „Wind Energy Extraction by Birds and Flight Vehicles", *AIAA Paper, AIAA 2005-0241*, American Institute of Aeronautics and Astronautics, 2005.

[18]Sachs, G., „Minimalbedingungen für den dynamischen Segelflug", *Zeitschrift für Flugwissenschaften und Weltraumforschung*, Vol. 13, pp.188-198, 1989.

[19]Sachs, G., Knoll, A., Lesch, K., "Optimal Control for Maximum Energy Extraction from Wind Shear", *AIAA Guidance, Navigation and Control Conference*, AIAA Paper 89-3490, 1989.

[20]Sachs, G., Knoll, A., Lesch, K., "Optimal utilization of wind energy for dynamic soaring", *Technical Soaring*, Vol. 15, No. 2, pp. 48-55, 1991.

[21]Sachs, G., "Optimal Wind Energy Extraction for Dynamic Soaring", *Applied Mathematics in Aerospace Science and Engineering*, Plenum Press, New York and London, Vol. 44, pp. 221-237, 1994.

[22]Sachs, G., Mayrhofer, M., "Shear Wind Strength Required for Dynamic Soaring at Ridges", *Technical Soaring*, ISSN 0744-8996, Band 25, Nr. 4, October 2001, pp. 209-215, 2001.

[23]Wurts, J., "Dynamic Soaring", *S&E Modeler Magazine*, Vol. 5, August/ September, pp. 2-3, 1998.

[24]Fogel, L., "Dynamic Soaring?", *S&E Modeler Magazine*, Vol. 9, December/January, pp. 4-7, 1999.

[25]Schlösser, W.M.J., "A Contribution to the Study of Dynamic Soaring", *S&E Modeler Magazine*, Vol. 5, March 2000, pp. 4-7, 2000.

[26]Sachs, G., Mayrhofer, M., "Dynamic Soaring Basics: Part 1 "Model Gliders at Ridges"", *Quiet Flyer*, ISSN 1532-3803, December 2002, pp. 32-37, 2002.

[27]Sachs, G., Mayrhofer, M., "Dynamic Soaring Basics: Part 2 "Minimum Wind Strength"", *Quiet Flyer*, ISSN 1532-3803, January 2003, pp. 82-85, 2003.

[28]Swolinsky, M., „Beiträge zur Modellierung von Scherwind für Gefährdungsuntersuchungen", *Dissertation*, TU Braunschweig, 1986.

[29]Weber, F., "Jet Stream and Clear-Air-Turbulence", *Aerokurier* 1/1968, pp. 20-21, 1968. http://squall.sfsu.edu/crws/jetstream.html.

[31]Köhler, H., Köhler, I., „Fly High – Segelfliegen in den USA", Verlag Dr. Neufang KG, Gelsenkirchen-Buer, 1984.

[32]*U.S. Standard Atmosphere 1976*, Washington D.C., National Oceanic and Atmospheric Administration, National Aeronautics and Space Administration, United States Air Force, 1976.

[33]*N.N., ALTOS – Software User Manual*, Institut für Flugmechanik und Regelung, University of Stuttgart, August 1996.

[34]*N.N., GESOP (Graphical Environment for Simulation and Optimization)*, Softwaresystem für Bahnoptimierung, Institut für Robotik und Systemdynamik, DLR, Oberpfaffenhofen, 1993.

[35]http://etaaircraft.zoecom.com/index.htm

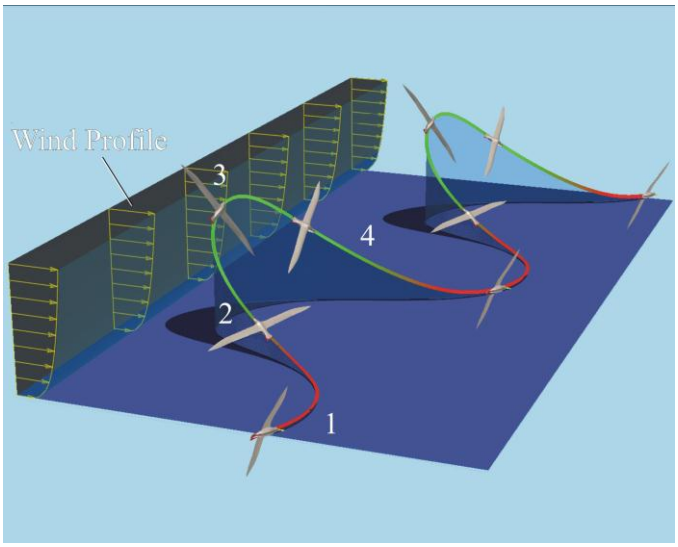

Figure 1 Dynamic soaring trajectory of albatross.

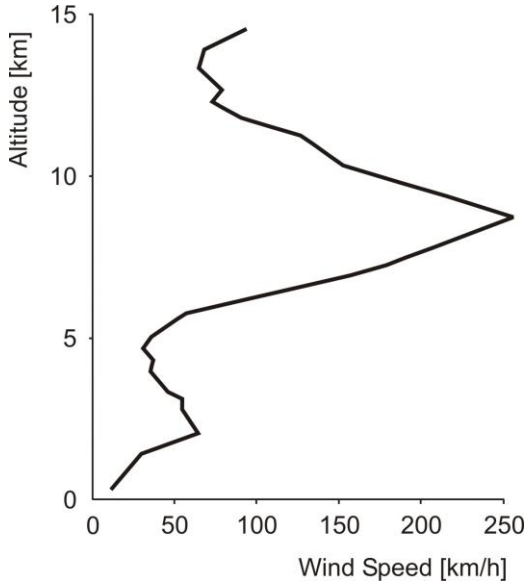

Figure 2 Shear wind associated with jet stream (data from Ref. 29).

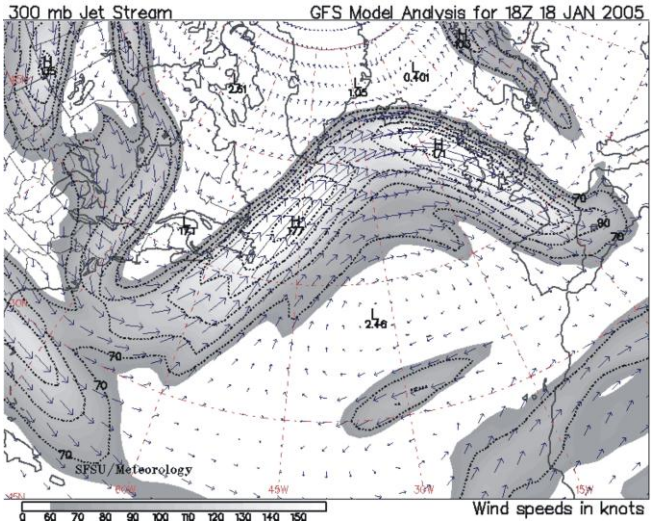

Figure 3 Extension of a jet stream (from Ref. 30).

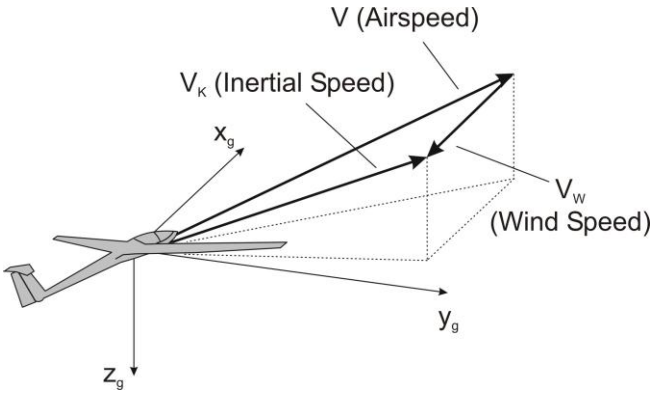

Figure 4 Geodetic coordinate system and speed vectors for flight of sailplane in horizontally moving air.

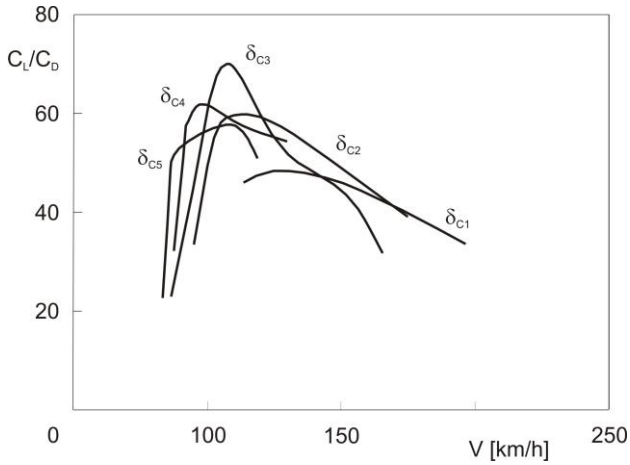

Figure 5 Lift-to-drag ratio of sailplane ($\delta_{C1}, \delta_{C2}, ..\delta_{C5}$: camber flap settings). Wing span: 30 m, wing area: 18.56 m^2.

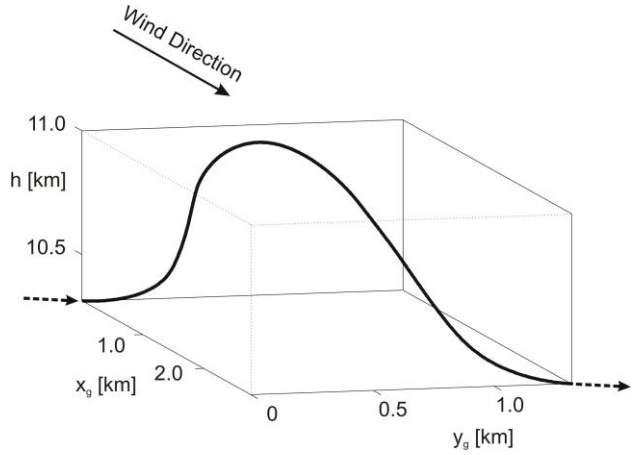

Figure 6 Optimal energy-neutral dynamic soaring cycle requiring minimum shear wind strength $(dV_W/dh)min=0.012\ s^{-1}$.

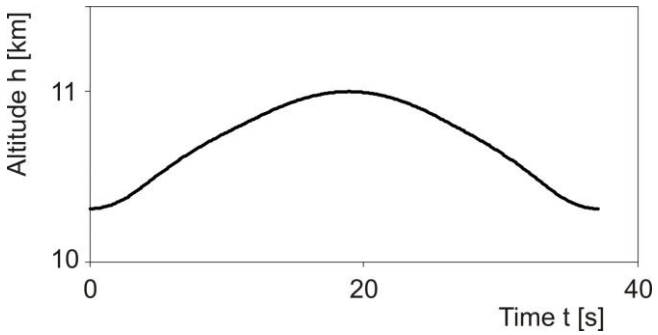

Figure 7 Altitude time history of optimal energy-neutral dynamic soaring cycle requiring minimum shear wind strength $(dV_W/dh)_{min}=0.012\ s^{-1}$.

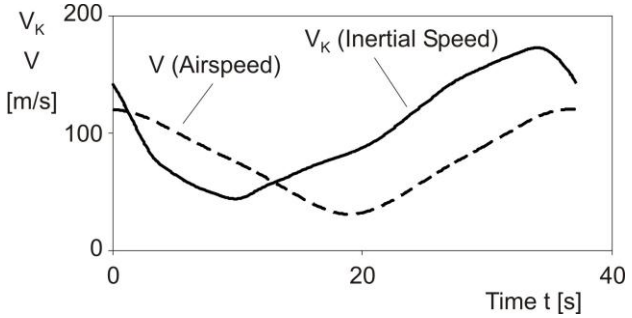

Figure 8 Speed time histories of optimal energy-neutral dynamic soaring cycle requiring minimum shear wind strength $(dV_W/dh)_{min}=0.012\ s^{-1}$

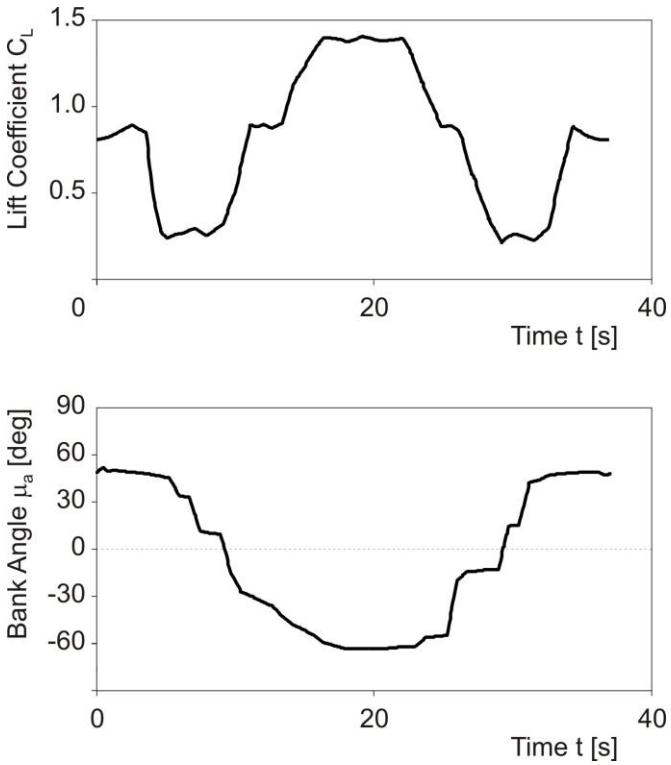

Figure 9 Time histories of lift coefficient and bank angle of optimal energy-neutral dynamic soaring cycle requiring minimum shear wind strength $(dV_W/dh)_{min}=0.012\ s^{-1}$.

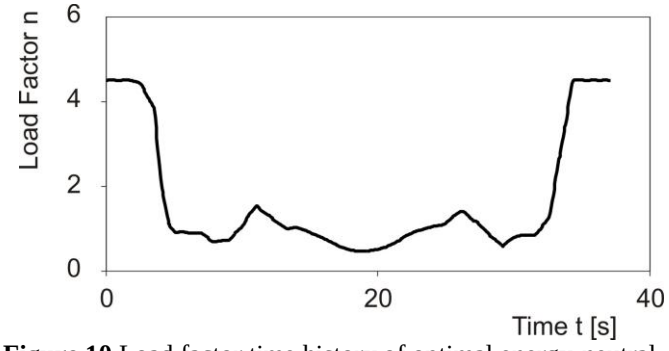

Figure 10 Load factor time history of optimal energy-neutral dynamic soaring cycle requiring minimum shear wind strength $(dV_W/dh)_{min}=0.012\ s^{-1}$.